

Migration and elimination characteristics of the self-interstitials in a Ag-30-at.-%-Zn alloy

M. Halbwachs, J. T. Stanley,* and J. Hillairet

Centre d'Etudes Nucléaires de Grenoble, Département de Recherche Fondamentale, Section de Physique du Solide,
85 X, 38041 Grenoble Cedex, France

(Received 4 January 1978)

A detailed analysis of the enhanced Zener ordering rate in a Ag-30-at.-%-Zn alloy has been carried out using elastic after-effect measurements for three conditions: (i) quasistationary state in a fast-electron flux, (ii) stationary state in a fast-electron flux, and (iii) upon suppression of the flux when steady-state regime prevailed. From a comparison of these results, the behavior of self-interstitial atoms has been investigated. The range 0.2–0.4 of the melting-point temperature was studied and in this range the jump frequency for the self-interstitials is $3 \times 10^{18} \exp[-0.94 \text{ (eV)}/kT]$ which is slower than that of the vacancies. Both self-interstitials and vacancies contribute to the ordering process and the extent of their contributions is discussed. It was found that dislocations were 10 times more efficient as sinks for interstitials than as sinks for vacancies. Some possible reasons for these unusual characteristics are put forward and discussed.

I. INTRODUCTION

In the preceding paper¹ (hereafter I), a study of the enhanced rate at which directional order is established in a Ag-30-at.-%-Zn alloy during 2.5-MeV electron irradiation led to the conclusion that the single vacancy in this alloy has a higher mobility than the self-interstitial. The purpose of the present paper is to analyze in more detail the fundamental characteristics of the self-interstitial, especially its absolute mobility, its interaction with dislocation sinks, and its ability to promote short-range ordering.

II. IRRADIATION RESULTS: COMPARISON OF QUASISTATIONARY AND STATIONARY RATES

Among other advantages, the in-flux measurements of elastic after-effect enable access, during a single irradiation run, to both the quasistationary and the stationary radiation-enhanced rates successively. In a flux of $4 \times 10^{11} \text{ e}^-/\text{cm}^2 \text{ sec}$, the following numerical values were obtained [I, Figs. (5) and (6)]:

$$\tau_{\text{st}}^{-1} (\text{sec}^{-1}) = 9480 \exp[-0.47 \text{ (eV)}/kT], \quad (1)$$

$$\tau_{\text{qst}}^{-1} (\text{sec}^{-1}) = 27.9 \exp[-0.28 \text{ (eV)}/kT]. \quad (2)$$

For the sake of comparison, in zero flux the thermal relaxation rate is

$$\tau_{\text{th}}^{-1} (\text{sec}^{-1}) = 2.5 \times 10^{14} \exp[-1.37 \text{ (eV)}/kT]. \quad (3)$$

Direct comparison of the quasistationary and stationary rates is of great interest. In fact, it gives valuable information about the relative mobilities of vacancies and self-interstitials, as can be seen by consideration of the expressions which describe the quasistationary and stationary ordering rates (I), i.e.,

$$\tau_{\text{st}}^{-1} = [\alpha_i \nu_i^* (\rho_v \nu_v / \rho_i \nu_i)^{1/2} + \alpha_v \nu_v^* (\rho_i \nu_i / \rho_v \nu_v)^{1/2}] \times [\sigma \epsilon \phi / Z (\nu_i + \nu_v)]^{1/2}, \quad (4)$$

$$\tau_{\text{qst}}^{-1} = (\alpha_i \nu_i^* + \alpha_v \nu_v^*) [\sigma \epsilon \phi / Z (\nu_i + \nu_v)]^{1/2}. \quad (5)$$

In these expressions, $\sigma \epsilon \phi$ is the production rate of freely migrating defects due to flux ϕ with efficiency equal to the product of the displacement cross section σ and the number ϵ of uncorrelated Frenkel pairs emitted by a primary knock-on. Z characterizes the spontaneous recombination of vacancies and self-interstitials, while ρ_v and ρ_i are the respective sink densities for these defects. The ordering rate is described by efficiency factors α and ordering jump frequencies ν^* . The ν 's are simply the defect mobilities. The only approximations are (i) the thermal vacancy concentration can be neglected compared with the concentration of vacancies created by irradiation, and (ii) defect losses at fixed sinks are not significant.

Then, without any further approximation, the ratio of the stationary to the quasistationary rates is

$$\frac{\tau_{\text{st}}^{-1}}{\tau_{\text{qst}}^{-1}} = \frac{\alpha_i \nu_i^* (\rho_v \nu_v / \rho_i \nu_i)^{1/2} + \alpha_v \nu_v^* (\rho_i \nu_i / \rho_v \nu_v)^{1/2}}{\alpha_i \nu_i^* + \alpha_v \nu_v^*}. \quad (6)$$

Two particular conditions are of special interest:

(i) The low-temperature range, in which the mobilities of vacancies and self-interstitials are very different. In this case, for nonzero α_i and $\nu_v \gg \nu_i$, the above ratio reduces to

$$\tau_{\text{st}}^{-1} / \tau_{\text{qst}}^{-1} = [(\rho_i / \rho_v) (\nu_i / \nu_v)]^{1/2}. \quad (7)$$

(ii) The temperature region in which τ_{qst}^{-1} approaches τ_{st}^{-1} , which implies $\rho_v \nu_v \approx \rho_i \nu_i$. Then two very distinct cases can occur, depending on the value of

ρ_i/ρ_v . First, assuming that dislocations are almost neutral sinks, the mobilities ν_v and ν_i for the two species tend to the same value (i.e., $\tau_{st}^{-1} = \tau_{st}^{-1}$) and then cross, leading to an inversion of mobilities at higher temperatures. Since the quasistationary and the stationary rates are systematically controlled by the faster and the slower-moving species, respectively, this inversion should result in an inversion of the activation energies and thus, a distortion of every one of the relevant curves. Alternatively, if dislocation sinks have a much higher efficiency for self-interstitials, the low-temperature relation $\nu_v \gg \nu_i$ is valid above the crossing point of the quasistationary and stationary curves, so that the deviation from linearity should be postponed to higher temperatures.

Thus, the ratio ρ_i/ρ_v is expected to influence significantly the temperature dependence of either curve. A parametric study is shown in Fig. 1 for the stationary curve. Also, the data points for both the quasistationary and the stationary conditions are presented. The quasistationary curve could not be extended to temperatures higher than 80 °C, as the time to reach the quasistationary condition is then too short. The stationary data were gained up to 140 °C, which means that the zone explored covers the region in which the curves cross, i.e., about 100 °C. Maximum accuracy is obtained for these temperatures because of the possible observation of the full-relaxation curves in a convenient period of time and therefore confidence in the numerical values of the parameters in this region is high. From the comparison of the theoretical and the experimental profiles in Fig. 1, the most probable value of ρ_i/ρ_v appears to be about 10. From this ratio, it can be inferred that the relative mobility of self-interstitials and vacancies is given by

$$\nu_i/\nu_v = 1.2 \times 10^4 \exp[-0.38(\text{eV})/kT]. \quad (8)$$

Alternatively, using $E_v^M = 0.56$ eV and $\nu_{0v} = 2.5 \times 10^{14}$ (from I),

$$\nu_i = 3 \times 10^{18} \exp[-0.94(\text{eV})/kT]. \quad (9)$$

This means in particular that the attempt frequency for self-interstitial migration is larger by four orders of magnitude than that of the vacancy. The numerical value of ρ_i/ρ_v will be discussed further in relation to other experimental results presented below.

III. POST-IRRADIATION STUDIES

This section deals with the decay of the radiation induced defect supersaturation on suppression of the flux. More precisely, the flux was cut off once the steady state was reached and the decay kinetics

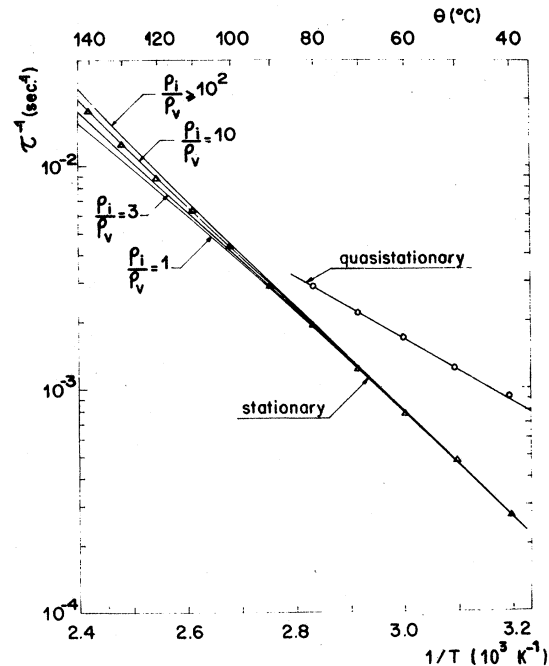


FIG. 1. Parametric study of the incidence of the ratio ρ_i/ρ_v on the stationary relaxation rate. The numerical values were: $\sigma\epsilon\phi = 5 \times 10^{-11}$ (displacements per atom) sec^{-1} ; $\nu_v = 2.5 \times 10^{14} \exp(-0.56(\text{eV})/kT)$; $\nu_i = 3 \times 10^{18} \times \exp(-0.94(\text{eV})/kT)$, for $\rho_i = \rho_v$; $Z = 18$ [16]. Calculation was performed with use of the full-balance expressions given by (6) and (7) in I. For the sake of comparison, the experimental data points have been reported for both the stationary and the quasistationary conditions.

were studied as a function of the annealing time. This type of experiment was conducted after low temperature irradiation, at 40 or 60 °C. A typical experimental run is shown in Fig. 2. The decay curve for the relaxation rate is found to be composed of an initial rapid decay and a subsequent slow evolution. This profile is satisfactorily accounted for by consideration of the general steady-state condition $\rho_i C_i \nu_i = \rho_v C_v \nu_v$, which, for $\nu_v \gg \nu_i$, implies that the stationary concentration of self-interstitials is much larger than the vacancy concentration. The initial period corresponds to the elimination of the minority of the fast species, the vacancy, either at sinks or by recombination. Then, after an appropriate aging time, only the interstitials remain in an almost unmodified concentration and subsequently anneal out. The elimination of these defects occurs solely by their annihilation at fixed sinks. Thus, this recovery is expected to obey first-order kinetics as verified in Fig. 3. It is interesting to note that the sink density of about $2 \times 10^{-9} \text{atom}^{-1}$ calculated from these data for the self-interstitials yields a value of $2 \times 10^{10} \text{atom}^{-1}$ for the vacancies, which is comparable to

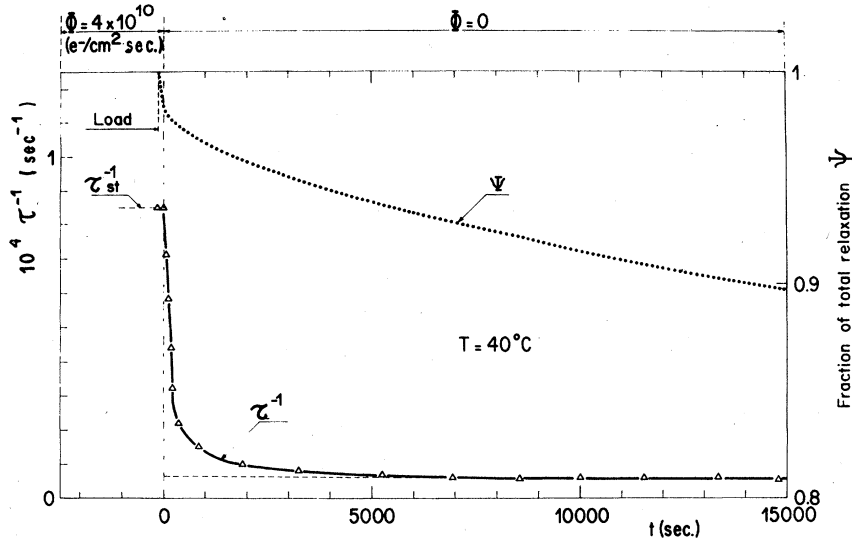


FIG. 2. Decay of the relaxation rate on suppression of a flux of $4 \times 10^{10} e^-/\text{cm}^2 \text{ sec}$. A prior irradiation for 2×10^5 sec. was chosen so that the steady-state regime was reached for the defect population.

the density inferred from the quenching studies [$(5 \text{ to } 7) \times 10^{-11} \text{ atom}^{-1}$] reported in I.

This type of experiment gives supplementary information about the effectiveness of the interstitialcy mechanism in the alloy under consideration, insofar as it enables the separation of the respective contributions of the two species to the ordering rate. Extrapolation of the final part of the decay curve to zero annealing time is a measure of the specific contribution of the self-interstitials in the stationary regime. The relevant numerical value at 40°C is about one-tenth of the total rate.

Considering Eq. (4), this ratio can be written

$$\frac{\tau_{st}^{-1}}{\tau^{-1}} = \frac{\alpha_i \nu_i^* (\rho_v \nu_v / \rho_i \nu_i)^{1/2}}{\alpha_i \nu_i^* (\rho_v \nu_v / \rho_i \nu_i)^{1/2} + \alpha_v \nu_v^* (\rho_i \nu_i / \rho_v \nu_v)^{1/2}} \approx \frac{\alpha_i}{\alpha_v} \frac{\rho_v}{\rho_i} \frac{\nu_v}{\nu_i^*} \frac{\nu_i^*}{\nu_i} \approx 0.1. \quad (10)$$

Since ν_i^* is not very different from ν_v , as was stated in I, and $\rho_i = 10\rho_v$,

$$\alpha_i / \alpha_v = \nu_i / \nu_i^*. \quad (11)$$

Hence, if $\nu_i^* \approx \nu_i$ then $\alpha_i = \alpha_v$. Conversely, if $\nu_i^* \ll \nu_i$ then $\alpha_i \gg \alpha_v$. The physical meaning of the α 's suggests that α_i lies between 0 and a value which should not be much larger than α_v .^{2,3} Thus, the most probable pair of relations is

$$\alpha_i \approx \alpha_v \text{ and } \nu_i^* \approx \nu_i. \quad (12)$$

The significance of this result is that an interstitial jump is about equivalent to a vacancy jump in producing directional order.

Consider now the initial portion of the decay. The steady-state conditions are such that the concentrations of vacancies and self-interstitials, as given by expressions (6) and (7) in I and numerical

values in the formulas (24) of I and (9) of this paper, are, respectively, 6.5×10^{-10} and $7.8 \times 10^{-9} \text{ atom}^{-1}$, while the sink density for vacancies is $7 \times 10^{-11} \text{ atom}^{-1}$ (I). Thus, since the concentration of self-interstitials is larger by at least two orders of magnitude than the effective sink density (for $Z=1$), it can be assumed that the mobile vacancies are annihilated primarily by encounter with relatively immobile self-interstitials. The concentration of the latter defect is altered only by 8%. Consequently, as a first approximation, c_i can be considered to be constant and the vacancy elimination kinetics should obey the first-order equation

$$\frac{dc_v}{dt} = -Z c_i c_v \nu_v \quad (13)$$

with a characteristic time $(Z c_i \nu_v)^{-1}$. From the

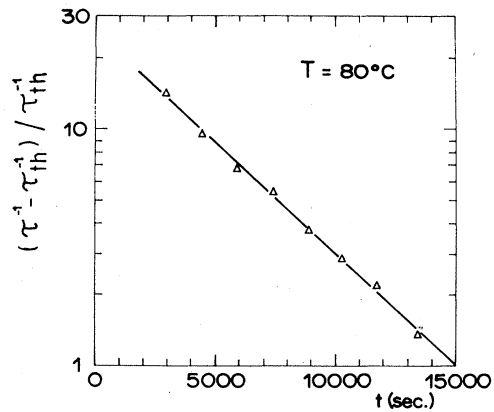


FIG. 3. Analysis of the final portion of the relaxation-rate decay. Conditions were the same as in Fig. 2, except that the irradiation temperature was 60°C and the annealing temperature 80°C . A good fit to first-order kinetics is observed.

above numerical values at 40 °C, this time is readily estimated to be 20 sec.

Figure 4 is a magnification of the initial part of a decay curve of the type presented in Fig. 2. This semilog diagram shows that the relaxation rate follows an exponential decay, from the moment the flux is suppressed. The measured characteristic time is 21 sec., which provides a satisfactory check of the self-consistency of all the numerical values involved.

IV. DISCUSSION

A. Efficiency of dislocations as sinks for point defects

Two rather unusual features were found in the Ag-30-at.%-Zn studied. On one hand, the average effective sink density is extremely small. It amounts, in carefully annealed specimens, to levels of about 10^{-10} atom $^{-1}$. On the other hand, it is shown in the present paper that a marked difference exists in the effective sink efficiency for vacancies and self-interstitials.

As a matter of fact, the elimination of point defects on dislocations involves complex mechanisms. Schematically, three successive steps can be defined: volume diffusion to the dislocation line, absorption by the dislocation core, and finally, either diffusion until a jog is reached, which results in the annihilation of the point defect by jog climb, or reemission. Most calculations for the dislocation sink density ρ are based on the solution of the diffusion equations for a regular array of hollow cylindrical sinks, with radii about equal to the radius r_c of the dislocation core. This scheme leads to the widely used formula⁴

$$\rho = 2\pi\delta a^2 / \ln(r_s/r_c), \quad (14)$$

with $\pi r_s^2 \delta = 1$. δ is the dislocation density and a is the lattice parameter. In this treatment a dislocation line is supposed to be a perfect collector. A more realistic model has been suggested by Baluffi,⁵ in which possible defect reemission is taken into account. The calculation for edge dislocations indicates that jogs can be described as ellipsoidal sinks, at the surface of which the defect concentration is in equilibrium with the jog. The minor axis of this ellipsoid is the capture radius, while its major axis W is given by

$$W = \sqrt{2} b \exp(\Delta E^M + \Delta E^B / kT). \quad (15)$$

b is the Burgers vector of the dislocation, ΔE^M the difference in the volume and pipe migration energies, and ΔE^B the defect-dislocation binding energy. Two cases can occur: (i) If the separation between jogs is lower than or equal to the ellipsoid length, the dislocation behaves like a perfect sink. Then the defect elimination is controlled by volume diffusion. This scheme leads to the previous result for a dislocation as a perfect collector. (ii) In the opposite case—insufficient pipe mobility, low jog density, low binding energy, or presence of a barrier to jog climb—the dislocations no longer act as perfect collectors, and the model becomes more intricate.

For many reasons, we are inclined to think that the Ag-Zn alloy belongs to this second class. The measured sink density of a few 10^{-11} atom $^{-1}$ for vacancies leads to a dislocation density of 10^4 cm $^{-2}$, using Eq. (14). This is an unrealistic value, which simply indicates that the condition of jog climb controlled by volume diffusion is not fulfilled. On

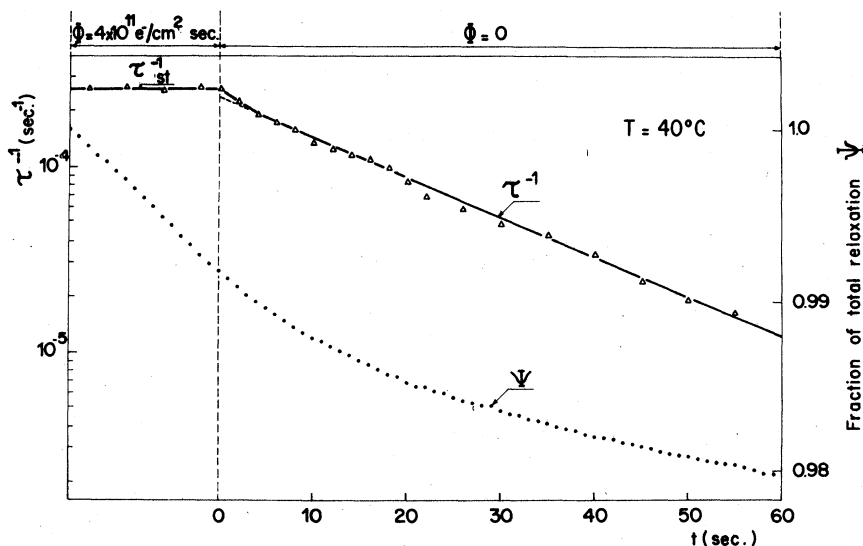


FIG. 4. Initial period of the decay curve on suppression of a flux 4×10^{11} e $^-$ /cm 2 sec, once a steady-state regime is reached. Annealing obeys first-order kinetics.

the other hand, the Ag-30-at.-%-Zn alloy has an unusually low stacking-fault energy, about 3 ergs/cm².⁶ Consequently the dislocations are expected to be strongly dissociated and the formation of jogs difficult.⁷⁻⁹ Recent calculations of the energy of dissociated jogs in a Cu-16-at.-%-Al alloy, which has a stacking-fault energy comparable to that of Ag-Zn (5 ergs/cm²), have led to values of about 58 eV.^{10,11} It is evident that the nucleation of jogs on such widely extended dislocations is difficult. Further, the diffusivity along an extended dislocation is smaller than along a perfect one.^{12,13} As a consequence the description of dislocations in Ag-Zn is as follows: (i) due to their marked dissociation, jogs are scarce; (ii) pipe and volume diffusivities are close to each other; (iii) since the jogs are also strongly dissociated, absorption of impinging defects is more difficult; (iv) as the dissociation partially relaxes the lattice, the elastic interaction energy is weaker and the defects are less strongly bound to the stacking fault ribbon.

In these conditions, once a defect has reached the dislocation line, a relatively long time passes before it reaches an efficient sink. This fact, together with the weaker binding, suggests that the defect has a higher probability to be reemitted. The sinks are then restricted to small volumes around the jogs and their density, within a given efficiency factor, is just the jog density. This explains the very small sink densities which were found in the Ag-Zn alloy. The second point refers to the different sink efficiencies of dislocations for vacancies and self-interstitials. The accepted scheme is that dislocations absorb the self-interstitials with a higher efficiency, because of the stronger elastic interactions between the dislocation and self-interstitial compared with the dislocation-vacancy interactions.^{14,15} This situation is generally described in terms of capture radii which are supposed to differ by 5% to 10%. If expression (14) is valid, this leads to a ratio ρ_i/ρ_v very close to unity. Thus such a model cannot yield a factor of 10, as found experimentally. Instead, high values can be obtained by considering the Balluffi model,⁵ in which elimination on a dislocation obeys the equation

$$\frac{dc_d}{dt} = -\frac{4\pi W}{\ln(2W/b)} \frac{\delta}{\chi} c_d \nu_d, \quad (16)$$

where c_d and ν_d are the relevant defect concentration and mobility. χ is the distance between jogs. Hence, the ratio of the effective sink densities is given by

$$\rho_i/\rho_v = \exp[(\Delta E_i^M + \Delta E_i^B) - (\Delta E_v^M + \Delta E_v^B)]/kT. \quad (17)$$

A difference of 0.08 eV in the activation energies at a mean temperature of 100 °C for this study re-

sults in a factor of 10 in the sink concentrations, thus providing a simple explanation for the marked difference in sink densities observed.

(In this calculation, the jog spacing χ was assumed to be constant. In fact, it is a function of the degree of supersaturation S [5] and the value of S depends on the ratio of the actual concentration of a given point defect to its thermal equilibrium value. Thus, if the formation energy of the interstitial is greater than the formation energy of a vacancy, the supersaturation due to interstitials will be greater than that due to vacancies and the jog spacing on the dislocations will be smaller; hence, the dislocations will behave as better line sinks for interstitials than for vacancies. This again could explain the differentiation which was observed experimentally.)

B. Migration characteristics of the self-interstitials

The self-interstitial was found to be less mobile than the vacancy. The two parameters which define its jump frequency, i.e., pre-exponential factor $3 \times 10^{18 \pm 1} \text{ sec}^{-1}$ and activation energy $0.94 \pm 0.02 \text{ eV}$ are both anomalously high. These high values suggest impurity trapping. Below, this effect is considered in some detail and subsequently ruled out. Then a possible retardation effect intrinsic to the alloy is considered.

1. Impurity trapping

The effects of a concentration of impurity trapping sites for self-interstitials on the build-up of the irradiation-produced defect concentrations were studied, using obvious modifications of the balance equations given in I, as follows:

$$\begin{aligned} \frac{dc_v}{dt} = & \sigma \epsilon \phi - \rho_v c_v \nu_v - Z c_t (c_v + c_{th}) (\nu_i + \nu_v) \\ & - Z c_t (c_v + c_{th}) \nu_v, \end{aligned} \quad (18)$$

$$\begin{aligned} \frac{dc_i}{dt} = & \sigma \epsilon \phi - \rho_i c_i \nu_i - Z c_t (c_v + c_{th}) (\nu_i + \nu_v) \\ & - Z_t c_t (c_t - c_c) \nu_i + c_c \nu_i \exp(E^B/kT), \end{aligned} \quad (19)$$

$$\begin{aligned} \frac{dc_c}{dt} = & Z_t c_t (c_t - c_c) \nu_i - c_c \nu_i \exp(-E^B/kT) \\ & - Z c_c (c_v + c_{th}) \nu_v, \end{aligned} \quad (20)$$

where c_t is the total trap concentration, c_c is the concentration of trapped interstitials, E^B is the binding energy of the interstitial-impurity complex, Z_t is the effective volume for trapping, and c_{th} is the vacancy concentration in thermodynamical equilibrium. It was assumed that each impurity can trap only one interstitial and that spontaneous

recombination volume with vacancies is the same for the trapped interstitial as for the free interstitial.

These equations were integrated numerically and the solutions were compared with the experimental results for a range of possible binding energies and interstitial migration energies. In fact, it turned out that the calculated mobility profiles versus temperature or time of irradiation could be equally well obtained from the original set of balance equations using an effective interstitial mobility $\bar{\nu}_i$ such that

$$\bar{\nu}_i = \nu_0 \exp(-E_i^M/kT) / [1 + Z_i c_i \exp(E^B/kT)]. \quad (21)$$

The calculation leads to a separation into two classes. For binding energies lower than 0.35 eV, the factor $Z_i c_i \exp(E^B/kT)$ is of the order of unity in the temperature range under investigation and distortions appear in both the build-up and decay irradiation profiles. This case can be excluded since the experimental curves do not exhibit any significant deviation from the estimated profiles at low temperature. On the other hand, for binding energies larger than 0.35 eV, the simulated curves are similar in every respect for both the intrinsic and the impurity case. The second term in the denominator of expression (21) is then much larger than unity, so that this expression simplifies to

$$\bar{\nu}_i = \nu_0 Z_i^{-1} c_i^{-1} \exp[-(E_i^M + E^B)/kT]. \quad (22)$$

In this case the temperature dependence for the effective defect mobility obeys the Boltzmann law, but with both pre-exponential factor and activation energy increased in comparison with the ideal, pure alloy. Thus, the unusually high migration energy found for the interstitial in this study can be attributed to a combined binding energy and motion energy. Moreover, the pre-exponential factor of 10^{18} sec^{-1} can be factored into a normal pre-exponential factor of approximately 10^{14} sec^{-1} and a factor $Z_i^{-1} c_i^{-1}$ of about 10^4 . If Z_i has about the same magnitude as the recombination volume for vacancies and interstitials, i.e., 18 (Ref. 16), then the required trap concentration is of the order of 10^{-5} . This is not an unreasonable number considering that the total impurity concentration in the alloy studied was about 40 ppm. Also the large implied binding energies are plausible, compared with the high values which were measured in several irradiated pure metals for undersized substitutional impurities.¹⁷⁻¹⁹

However, a very recent study on a less-concentrated Ag-Zn alloy²⁰ has shown that when the zinc concentration is decreased from 30 to 24 at.%, both the pre-exponential factor and the activation energy are markedly decreased, from 10^{18} to 10^{16} and from 0.94 to 0.82 eV, respectively. The value

of 10^{16} is of special interest. It corresponds in the impurity trapping model, to a product $Z_i c_i$ which is only 10^{-2} , and thus an impurity concentration of about $10^{-3} \text{ atoms}^{-1}$. Such a high impurity concentration can be ruled out for our specimens. As a consequence, we have to consider an intrinsic mechanism specific to the alloy system.

2. Influence of the alloying on the interstitial properties

For a discussion of interstitial mobility in binary alloys, there are two important questions to consider: (i) What changes are produced in mobility parameters by alloying? (ii) Does the interstitial migration produce changes in short-range order (interstitialcy mechanism)? With respect to the first question, it has been shown that a strong trapping is expected in dilute solid solutions when the solute atom is smaller than the solvent atom.¹⁹ Such is the case for zinc atoms dissolved in silver. In the particular case of the Ag-Zn system, several experimental observations have indicated that interstitials are indeed trapped by zinc atoms. From a study of the electrical resistivity recovery spectrum in dilute Ag-Zn alloys irradiated at low temperature, Ivanov *et al.*²¹ concluded that the interaction of the self-interstitials with zinc atoms was attractive but small. However, a stronger trapping effect exists in more concentrated (13.6 at. % - Zn) alloys.²² This led Rothman and Lam²³ to suggest the possibility that the self-interstitial might be bound more tightly to a small cluster of zinc atoms than to a single zinc atom. However, it is not clear how any of these ideas can be extended to highly concentrated alloys. Also it is not clear how these ideas can explain the unusually large pre-exponential factor that was measured. Composition fluctuations and/or ordering modulations can also be invoked, because of the proximity of the phase boundary for the alloy composition which was studied.

The situation is even more confusing with regard to the question of the interstitialcy mechanism. Here the basic principle is that the two types of atoms must be approximately equally capable of forming an interstitial. It has been stated without further justification that the change in ordering energy must be greater than the difference in formation energies of the two types of interstitials.^{24,25} However, it appears that the techniques for calculating the formation energies of interstitials are not sufficiently refined to be applied to concentrated alloys with any confidence. Experimentally, there is a scarcity of data on which to base a theory. The interpretation of the existing data has been controversial, especially in α brass.^{24,25} The present experiment is the first to give clear-cut

evidence that the interstitialcy mechanism is operative in a concentrated binary alloy with widely different component elements. This observation is taken as an indication that the interstitial configuration is quite different in the alloy from that in the pure metal.

V. CONCLUSION

The above analysis indicates that the marked reduction of the interstitial mobility from the high migration rate generally observed in pure metals is an intrinsic alloying effect in the Ag-30-at.-%-Zn alloy. It was found also that the interstitialcy mechanism was operative, although the component elements in this alloy have very different atomic sizes. Finally, a unique property of the alloy is that dislocations act as *much more* efficient sinks

for self-interstitials than for vacancies. This is attributed to widely dissociated dislocations, which occur as a consequence of an exceptionally low stacking-fault energy in the alloy.

ACKNOWLEDGMENTS

The authors wish to thank Dr. Y. Adda and Professor A. Seeger for their interest in this work. They gratefully acknowledge Dr. R. W. Carpenter and G. J. Dienes for stimulating discussions on the problem of defect mobility in alloys and Dr. A. Bourret and Professor P. Guyot for helpful suggestions on various aspects of point defect-dislocation interactions. They are indebted to Dr. I. G. Ritchie for a critical reading of the manuscript and to G. Casali for his valuable assistance with the experimental measurements.

*Visiting scientist from Arizona State University, Tempe, Ariz. 85281.

¹M. Halbwachs and J. Hillairet, Phys. Rev. B 18, 4927 (1978).

²S. Radelaar, Proceedings of the International Conference on Vacancies and Interstitials in Metals, Jülich, Germany, 1968, edited by A. Seeger, D. Schumacher, W. Schilling, and J. Diehl (unpublished), p. 667.

³A. Caplain and W. Chambron, Acta Metall. 25, 1001 (1977).

⁴F. J. Ham, J. Appl. Phys. 30, 915 (1959).

⁵R. W. Balluffi, Phys. Status Solidi 31, 443 (1969).

⁶A. Howie and P. R. Swann, Philos. Mag. 6, 1215 (1961).

⁷R. M. Thomson and R. W. Balluffi, J. Appl. Phys. 33, 803; 33, 817 (1962).

⁸J. Friedel, Dislocations (Pergamon, Oxford, 1964), Chap. VI.

⁹J. P. Hirth and J. Lothe, *Theory of Dislocations*, (McGraw-Hill, New York, 1968), p. 531

¹⁰D. J. H. Cockayne (private communication in Ref. 9).

¹¹T. Kosel and J. Washburn, *Fundamental Aspects of Radiation Damage in Metals*, (National Technical In-

formation Service, Springfield, Va., 1975), p. 903.

¹²R. W. Balluffi, Phys. Status Solidi 42, 11 (1970).

¹³R. W. Balluffi, in Ref. 11, p. 852.

¹⁴R. Bullough, Nucl. Appl. Technol. 9, 346 (1970).

¹⁵P. T. Heald, Philos. Mag. 31, 551 (1975); Acta Metall. 23, 1389 (1975).

¹⁶M. Halbwachs, J. Hillairet, and J. R. Cost, J. Nucl. Mater. 69, 776 (1978).

¹⁷H. Wollenberger, in Ref. 11, p. 582.

¹⁸M. L. Swanson in Ref. 16, p. 372 and p. 744.

¹⁹W. Schilling, in Ref. 16, p. 465.

²⁰D. Béretz and M. Halbwachs (unpublished).

²¹L. I. Ivanov, Yu. M. Platov, M. N. Pletnev and S. I. O. Sadykhov, in Ref. 16, p. 754.

²²Yu. M. Platov, M. N. Pletnev, V. I. Popov, and S. I. O. Sadykhov, Fiz. Met. Metalloved. 39, 1290 (1975).

²³S. J. Rothman and N. Q. Lam, Phys. Status Solidi A 35, K13 (1976).

²⁴A. C. Damask, J. Gilbert and H. Herman, Radiat. Eff. 26, 89 (1975).

²⁵K. Salamon and W. Schüle, Radiat. Eff. 16, 45 (1972).